Est. 1984

ORIENTAL JOURNAL OF CHEMISTRY

An International Open Access, Peer Reviewed Research Journal

www.orientjchem.org

ISSN: 0970-020 X
CODEN: OJCHEG
2023, Vol. 39, No.(6):
Pg. 1675-1682

"Synthesis, Characterization, and Applications of Y_2O_3 Nanoparticles Synthesized via, Thermal Decomposition of the [$Y(Cup)_2(Gly)\cdot 2H_2O$] Complex"

VISHAL S. KAMBLE[1], SUNIL S. PATIL[1], SAGAR L. KHAIRNAR[1], DIGAMBAR K. PATIL[1], SATYAJIT S. KAMBLE[1], SAPANA M. CHILATE[1] and JITENDRA M. PAWARA[1]*

[1]Changu Kana Thakur Arts Commerce and Science College (Autonomous), New Panvel, Maharashtra, India.
*Corresponding author E-mail: jmpawara@gmail.com

http://dx.doi.org/10.13005/ojc/390630

(Received: October 07, 2023; Accepted: November 18, 2023)

ABSTRACT

This research paper presents the synthesis and characterization of a novel Yttrium (III) complex. This complex consists of yttrium chloride hexahydrate coordinated with two primary ligands: (2Z)-2-(N-hydroxyimino)-1,2-diphenylethan-1-ol (Cupron) and glycine as the secondary ligand. The complex, denoted as [$Y(Cup)_2(Gly)\cdot 2H_2O$], underwent thorough characterization using various analytical techniques, including elemental analysis, infrared spectroscopy (IR), ultraviolet-visible spectroscopy (UV-Vis), and differential thermal/thermogravimetric analysis (TG/DTA). A noteworthy observation was made during the thermal decomposition of the complex at a relatively low temperature of 400°C. This process yielded pure Yttrium oxide (Y_2O_3) nanoparticles with a consistent spherical particle morphology. The structural analysis of these Y_2O_3 nanoparticles was carried out through Fourier-transform infrared spectroscopy (FT-IR), ultraviolet-visible spectroscopy (UV), thermogravimetric analysis (TG/DTA), X-ray diffraction (XRD), scanning electron microscopy (SEM), and transmission electron microscopy (TEM). Of particular significance is the antimicrobial activity exhibited by the synthesized Yttrium oxide nanoparticles. This observation suggests promising applications for these nanoparticles as potential antimicrobial agents or materials.

Keywords: Yttrium complex, Yttrium oxide nanoparticles, Antimicrobial activity.

INTRODUCTION

The synthesis of nanoparticles has emerged as a fascinating field of research with numerous applications in various scientific and technological domains. Yttrium oxide nanoparticles have gained considerable interest among various nanoparticles, thanks to their distinctive properties and promising utilization in diverse domains, including electronics, catalysis, biomedical engineering, and energy storage.[1] Yttrium oxide (Y O) is a binary compound composed of yttrium, a rare earth metal, and oxygen. The synthesis of yttrium oxide nanoparticles involves the controlled fabrication of these particles at the nanoscale, typically ranging from 1 to 100 nanometers in size.[2]

Yttrium oxide nanoparticles exhibit a spectrum of favorable attributes, encompassing high thermal stability, superb chemical resistance, and low electrical conductivity. These attributes make them highly suitable for diverse applications, including solid-state electrolytes in fuel cells, luminescent materials in displays and lighting devices, and as additives for enhancing the mechanical and thermal properties of materials. Furthermore, their unique optical, electronic, and magnetic properties offer potential in areas such as photonics, optoelectronics, and magnetic data storage.[3]

Various methods have been developed to synthesize yttrium oxide nanoparticles, each with its own advantages and limitations. Common techniques include sol-gel synthesis, thermal decomposition, precipitation, hydrothermal synthesis, and aerosol processes. These methods enable the controlled formation of yttrium oxide nanoparticles with tailored sizes, shapes, and surface properties, allowing researchers to optimize their properties for specific applications.[4]

In this article, we will explore the synthesis of yttrium oxide nanoparticles in detail, discussing the principles behind different synthesis methods and highlighting their respective advantages and challenges. We will delve into the key parameters that influence the size, shape, and properties of the nanoparticles, such as precursor materials, reaction conditions, and post-synthesis treatments. Additionally, we will explore the characterization techniques employed to analyze the structure, morphology, and composition of yttrium oxide nanoparticles.

By understanding the synthesis techniques and properties of yttrium oxide nanoparticles, researchers can further advance their applications across various fields. The ability to engineer nanoparticles with precise control over their characteristics opens up new avenues for innovation and exploration in nanotechnology, leading to advancements that can revolutionize industries and contribute to scientific progress.

EXPERIMENTAL

Materials

The chemicals employed in the synthesis of mixed ligand complexes were purchased from E. Merck Pharma. Yttrium chloride hexahydrate and the amino acid L-glycine were used without purification for the synthesis of metal complexes. The primary ligand, Cupron, was also utilized in the complex synthesis. Solvents such as DMF, DMSO, ethanol, and acetone were used in the research work after distillation and purification following standard protocols for complex synthesis. Analytical balance and Borosil glasswares were used, and standard calibration protocols were followed for accurate measurements.

Physical Measurements

In the course of this study, several analytical techniques and instruments were employed. Elemental analysis, encompassing the determination of carbon (C), hydrogen (H), and nitrogen (N) content, was executed at IIT Mumbai using a Thermo Finnigan Elemental Analyser with model number FLASH EA 1113 series. Yttrium content estimation was accomplished through complexometric analysis, following established protocols. Fourier Transform Infrared (FT-IR) spectra were meticulously recorded in the spectral range of 4000-400 cm^{-1}, utilizing a Perkin Elmer Spectrum FT-IR instrument with model number 1500. UV-Vis spectra were captured using a Perkin Elmer Lambda-950 UV-Vis spectrometer, with dimethyl sulfoxide (DMSO) as the solvent, spanning the wavelength range from 200 to 800nm. Thermal analysis was carried out under controlled nitrogen atmosphere, employing a Perkin Elmer Diamond TG-DTA instrument. Furthermore, to characterize the Yttrium oxide nanoparticles synthesized in this study, scanning electron microscopy (SEM) was conducted with a Hitachi S-4800 instrument, and X-ray diffraction (XRD) analysis was performed using a Bruker D 8 Advance X-ray diffractometer.

Synthesis of Mixed Ligand Yttrium (III) Complexes

To prepare the complex, we initiated the process by blending an aqueous solution of yttrium chloride hexahydrate (303 mg, 1 mmol) with 10 mL of an alcoholic solution of (2Z)-2-(N-hydroxyimino)-1,2-diphenylethan-1-ol (454 mg, 2 mmol) while ensuring continuous stirring. This mixture was subsequently subjected to heating in a water bath for 10-15 minutes. Following this step, we added an aqueous solution of amino acids (1 mmol) drop by drop into the reaction mixture, maintaining continuous stirring. The entire mixture was once again heated, this time

in a boiling water bath, for an additional 10 minutes. After the heating process, we carefully transferred the reaction mixture to an asbestos sheet, and in a precise manner, introduced dilute ammonia solution drop by drop into the beaker. The formation of the complex became evident as the pH gradually increased upon the addition of ammonia solution. The resulting solution, which contained the complex precipitate, was then efficiently filtered through a Buchner funnel, and the solid complex underwent thorough washing with ethyl alcohol and water before being subjected to drying in an oven.[5]

Synthesis of nanoparticles by thermal decomposition of Y(III) complex

Approximately 0.5 g of a newly synthesized Y(III) complex underwent a thermal decomposition process within an oven, maintained at a temperature of 400°C for a duration of 30 minutes. This thermal treatment yielded a powder with an off-white hue, indicating the successful production of Yttrium oxide (Y_2O_3) nanoparticles. Subsequently, the resultant powder was allowed to naturally cool to room temperature, followed by meticulous washing with ethanol multiple times to eliminate any lingering impurities. Ultimately, the prepared Y_2O_3 nanoparticles were subjected to an oven-drying process, resulting in the attainment of a dry and stable form. This synthesis method effectively facilitated the conversion of the Y(III) complex into Yttrium oxide nanoparticles, thereby paving the way for further characterization and potential applications.[6]

Biological activity

Agar Cup Method

In this method, a 1000 mL solution of Mueller Hinton Agar (MHA) is prepared using distilled water and sterilized at 121°C for 20 minutes. After sterilization, it is allowed to cool down to 40°C. All glassware used in the experiment is sterilized as well. An 18-hour-old bacterial culture with a density of 10^6 cells/cm^3 is incubated in the Mueller Hinton Agar, and 20 cm^3 of the agar is poured into sterile plates, which are then cooled and allowed to solidify. Each plate is punctured with three wells of 8 mm diameter. Tetracycline (0.1 cm^3) is used as a control. The wells are filled with 0.1 cm^3 solutions of the prepared complexes in DMSO, labeled with the sample names. The sterile plates are then incubated for 24 hours at 37°C, and the zones of inhibition are measured to determine the antibacterial activity of the complexes.[7-9]

Tube Dilution Method

To find the Minimum Inhibitory Concentration (MIC) of the complexes, the tube dilution method is employed. Stock solutions of all complexes in DMSO are prepared at a concentration of 1 mg/cm^3, and further dilutions are made. The bacterial culture stock is also diluted with sterile broth to achieve a concentration of 10^6 cells/cm^3. Four sets of sterile tubes are taken for each bacterial strain and labeled with various concentrations of the prepared complexes. Each sterile tube is filled with 5 cm^3 of the diluted solution of the yttrium complexes, and the diluted bacterial culture is added to each tube. The tubes are then sealed and incubated for 24 h at 37°C. Tetracycline is used as the standard. Positive controls are maintained by incubating 5 cm^3 sterile Mueller Hinton Broth with bacterial culture. Additionally, 5 cm^3 DMSO of 10^{-3} M dilution in three tubes are kept for each bacterial strain to observe bacterial growth. The tubes are examined for turbidity, and the minimum inhibitory concentration is determined by the absence of visible change in turbidity.[10-13]

Table 1: Antibacterial activity by Agar Cup Method

S. No	Complex	Antibacterial activity (mm)			
		S.aureus	*C. diphtheriae*	*S. typhi*	*P. aeruginosa*
1	$[Y(Cup)_2(Ala)\cdot 2H_2O]$	16	13	8	9
2	Y_2O_3	20	18	12	14
--	Tetracycline	30	23	25	16

Table 2: Data of Antibacterial activity by Tube Dilution Method

S. No	Complex	MIC (µg/cm^3)			
		S. aureus	*C. diphtheriae*	*S. typhi*	*P. aeruginosa*
1	$[Y(Cup)_2(Ala)\cdot 2H_2O]$	70	75	100	117
2	Y_2O_3	80	82	118	100

Table 3: MIC of Metal Salts, Ligand and Tetracycline by Tube Dilution Method

Salt/Ligand/Tetracycline	MIC (µg/cm³)			
	S. aureus	*C. diphtheriae*	*S. typhi*	*P. aeruginosa*
$Y.Cl_3.6H_2O$	100	140	1450	180
Cupron	100	200	150	140
Tetracycline	1.5	2.0	1.5	7.0

The antibacterial activity data presented in Tables 2 and 3 reveal insights into the inhibitory potential of the tested compounds against various bacterial strains. Table 2 indicates that both the $[Y(Cup)_2(Ala)\cdot 2H_2O]$ complex and Y_2O_3 nanoparticles exhibit moderate antibacterial activity, with smaller inhibition zones compared to the standard tetracycline. Table 3 demonstrates the Minimum Inhibitory Concentration (MIC) values, with lower values indicating stronger inhibition. Here, $[Y(Cup)_2(Ala)\cdot 2H_2O]$ complex showcases better inhibitory potential compared to Y_2O_3 nanoparticles. Tetracycline exhibits the lowest MIC values, displaying potent antibacterial action. In summary, the data underscores the varying antibacterial efficacy of the tested compounds. While tetracycline stands out with strong inhibition, the tested complexes and Y_2O_3 nanoparticles display moderate antibacterial activity.

RESULTS AND DISCUSSION

This Chapter study mainly focused on the preparation of mixed ligand Yttrium complexes, study of their physicochemical properties and spectral interpretation of Yttrium(III) complexes.

$$YCl_3\cdot 6H_2O + 2HCup + HL \longrightarrow [Y(Cup)_2(L)\cdot 2H_2O] + 3HCl + 4H_2O$$

$$[Y(Cup)_2(L)\cdot 2H_2O] \xrightarrow{\text{Thermal Decomposition}} Y_2O_3 \text{ Nanoparticles}$$

Where,
HCup : Cupron
HL : Amino acid

Where HCup represents (2Z)-2-(N-hydroxyimino)-1,2-diphenylethan-1-ol, and HL corresponds to alanine. The resulting complex exhibits a light white color, possesses non-hygroscopic properties, and stands as a thermally stable solid, signifying the presence of strong metal-ligand bonds. This complex demonstrates partial solubility in various solvents, including methanol, ethanol, chloroform, DMF, and DMSO. The elemental analysis data for the metal complex aligns with a general formulation of 1:2:1, indicative of a complex of the form $[Y(Cup)_2(L)\cdot 2H_2O]$. Furthermore, when the complex is dissolved in DMF at a concentration of 10^{-3} M, its molar conductance values are consistently low (<1), suggesting its non-electrolytic nature.[14-15]

UV Spectra

In methanol, the electronic spectra of the metal complex, recorded in the UV region, reveal the presence of intra-ligand and charge transfer transitions. Specifically, three distinct transitions are discernible: one at 203-263 nm ($n\rightarrow\pi^*$), another at 337 nm ($\pi\rightarrow\pi^*$), and a third in the range of 384-386 nm, signifying a charge transfer from ligands to the metal center. In chloroform, the spectra of the metal comple2xes in the visible region display a notable charge transfer transition occurring at 400-420nm. Furthermore, additional transitions manifest at 560-600nm and 820-840nm, characteristic of d-d transitions commonly observed in transition metal complexes. It is noteworthy that the UV-Vis spectrum of Y_2O_3 nanoparticles differs significantly from that of the initial complex. This divergence confirms that the 288nm band originates from the Y_2O_3 nanoparticles and not from the Y(III) complex. Importantly, the UV-Vis spectrum of commercially available bulk Y_2O_3 powder does not display any discernible absorption bands.[16-17]

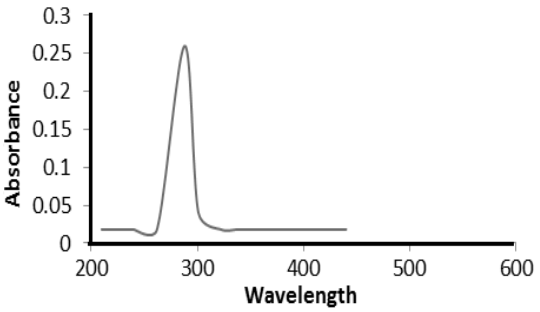

Fig. 1. UV spectra of Y_2O_3 nanoparticles

FTIR Spectra

The IR spectrum displays distinctive absorption bands between 3400-3600, 2940,

3238, 1267-1212, 600-590, and 510 cm^{-1}. These correspond to coordinated-H_2O, -NH_2, CO, N-O, and M-N stretching vibrations, respectively. After thermal decomposition at 400°C, the specific bands related to the HCup and HL compounds vanish. Instead, a robust 440 cm^{-1} band arises, attributed to Y–O stretching in Y_2O_3 NPs.[18]

SEM

Figure 2 displays SEM micrographs illustrating the Y(III) complex and its resulting decomposition product at 400°C. A discernible transformation is evident in these images. The initial complex powder, as depicted in Fig. 2a, consists of substantial block crystals varying in size. In stark contrast, the SEM image of the product (Fig. 2b) vividly showcases particles with distinct shape and size characteristics compared to the precursor complex. The product's SEM image reveals the presence of exceedingly fine semi-spherical particles, loosely aggregated in nature. Notably, the product's morphology stands in stark contrast to that of the complex, indicating a significant shift in structure during decomposition. The absence of characteristic morphological traits from the complex further underscores the completion of decomposition, resulting in the formation of these finely textured spherical particles. This visual evidence reinforces the profound alteration from large block crystals to delicately structured, loosely aggregated particles.[19-20]

TEM

Illustrated in Fig. 3 are the TEM images depicting both the complex and its resultant decomposition product at 400°C. Initial observations reveal that the TEM micrograph of the initial complex powder (Fig. 3a) is dominated by large block crystals of varying dimensions. Conversely, the thermal decomposition process yields uniformly shaped Y_2O_3 nanoparticles (Fig. 3b), exhibiting spherical morphology with mild agglomeration. Upon decomposition, the particle size distribution demonstrates a remarkable uniformity, spanning from 8 to 12nm, and culminating in an average particle diameter of approximately 10nm. Notably, this average particle size, as determined through TEM analysis, closely mirrors the previously computed value attained through alternative methods. This concurrence underscores the reliability and consistency of the particle size estimation technique employed. The TEM images distinctly capture the metamorphosis from bulky crystalline structures to finely defined nanoparticles, providing visual confirmation of the successful synthesis and ensuing decomposition process.[21-22]

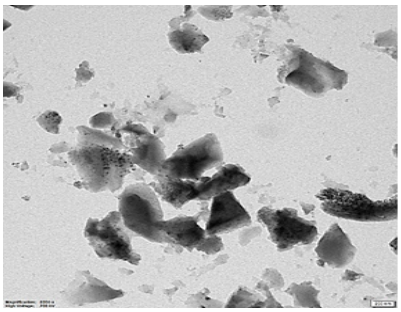

Fig. 2(a). SEM image Y(III) complex

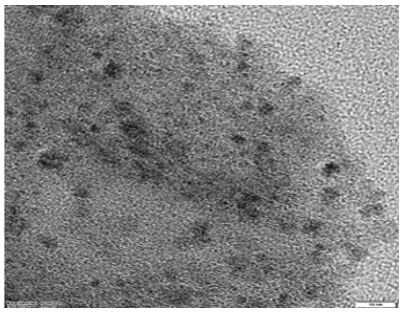

Fig. 2(b). SEM image of Y_2O_3 nanoparticles

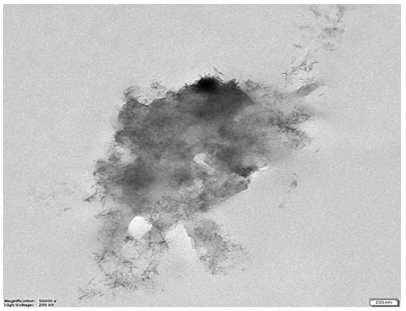

Fig. 3(a). TEM image Y(III) complex

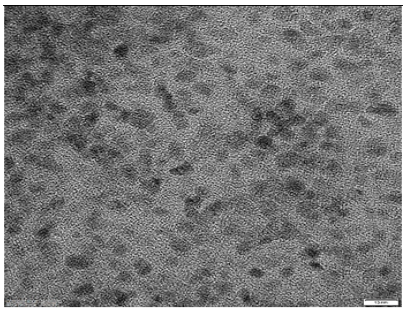

Fig. 3(b). TEM image of Y_2O_3 nanoparticles

XRD

Y_2O_3 powders were synthesized utilizing a modified thermal decomposition process conducted at 400°C for a duration of 30 minutes. The crystal structure and morphology of the resulting Y_2O_3 nanoparticles were comprehensively characterized

employing X-ray diffraction (XRD), thermogravimetric analysis with differential scanning calorimetry (TG-DSC), and field-emission scanning electron microscopy (FE-SEM). The XRD pattern unveiled four distinctive, strong, and broad peaks occurring at 2θvalues approximately equal to 29.2, 33.8, 48.5, and 57.60 degrees. These peaks corresponded to the (222), (400), (440), and (622) reflections of cubic Y_2O_3, respectively, as per the JCPDS card number 89-5591. Additionally, the determination of the average Y_2O_3 nanoparticle size was accomplished employing the Debye-Scherrer equation, based on the relative intensity peak (222), resulting in an estimated size of approximately 10nm. The increased sharpness of the XRD peaks signifies the crystalline nature of the particles. The calculation formula employed for this determination is as follows:

$$D = (0.94\lambda)/(\theta\cos\theta)$$

In the above formula, λ denotes the X-ray wavelength (λ=1.542 Å) corresponding to Cu-Kα radiation, β signifies the full width at half maximum (FWHM) of the diffraction line, and θ represents the diffraction angle. The utilization of this analytical approach offers valuable insights into the structural and size attributes of the Y_2O_3 nanoparticles. Such insights prove instrumental in comprehending the potential applications of these nanoparticles across various fields.[24-25]

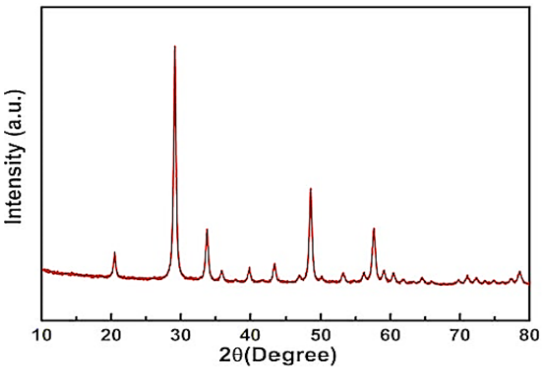

CONCLUSION

In conclusion, the comprehensive analysis of Y_2O_3 nanoparticles and the Y(III) complex has yielded valuable insights into their structural, electronic, and morphological properties. Electronic spectra in methanol unveiled distinct transitions: 203-263nm (n→π*), 337 nm (π→π*), and 384-386nm (charge transfer). In chloroform, a charge transfer transition at 400-420nm, along with d-d transitions at 560-600nm and 820-840nm, indicated the complex's solvent-dependent behaviour. The UV-Vis spectrum of Y_2O_3 nanoparticles distinctly differed from the initial complex, confirming the source of the 288nm band. FTIR analysis revealed shifts in absorption bands after decomposition: coordinated-H_2O, -NH_2, CO, N–O, and M–N stretching vibrations. SEM images depicted the transformation from large block crystals in the complex to finely shaped, semi-spherical particles in the product. TEM analysis further supported this transformation, with particle sizes averaging around 10nm post-decomposition. XRD patterns validated the crystalline nature of the nanoparticles, with strong peaks at 2≈29.2, 33.8, 48.5, and 57.60 corresponding to (222), (400), (440), and (622) reflections of cubic Y_2O_3, respectively. This structural information aligns with the uniformity observed in the TEM images. Collectively, these results provide a comprehensive understanding of the synthesis, decomposition, and properties of Y_2O_3 nanoparticles, offering numerical evidence to guide their potential applications in various fields.

The conducted antibacterial activity assays highlight the moderate inhibitory potential of the $[Y(Cup)_2(Ala)\cdot 2H_2O]$ complex and Y_2O_3 nanoparticles against bacterial strains. While these substances demonstrate promising activity, their efficacy is notably surpassed by the standard antibiotic tetracycline.

ACKNOWLEDGEMENT

The author Dr. Jitendra M. Pawara extends gratitude to Changu Kana Thakur Arts, Commerce & Science College (Autonomous), New Panvel, Navi Mumbai. The college provided instrumental and laboratory resources, along with research funding through the 'RUSA grant Scheme of Seed Money for Research to Teacher Rashtriya Uchchatar Shiksha Abhiyan, enabling the completion of this research work.

Conflict of interest

The authors declare that there are no conflicts of interest related to this research work.

REFERENCES

1. Vennila R.; Kamaraj P.; Sridharan M.: Arockiaselvi J.; Green synthesis, characterization of yttrium oxide, stannous oxide, yttrium doped tin oxide and tin doped yttrium oxide nanoparticles and their biological activities. *Materials today*., **2021**, *36*(4), 920-922. https://doi.org/10.1016/j.matpr.2020.07.032
2. Bharat L. K.; Goli N.; Kurugundla G. K.; and Jae S. Y.; Controlled synthesis of yttrium gallium garnet spherical nanostructures modified by silver oxide nanoparticles for enhanced photocatalytic properties. *Cry. Eng. Comm*., **2016**, *18*, 8915-8925 https://doi.org/10.1039/c6ce01988a
3. Qian L.; Lining C.; Junyan T,; Xuezhi L.; Junjie L.; Mi T.; Zhengbang W.; Large-scale preparation of ultrathin composite polymer electrolytes with excellent mechanical properties and high thermal stability for solid-state lithium-metal batteries *Energy Storage Materials.,* **2023**, *55*, 847-856, https://doi.org/10.1016/j.ensm.2022.12.039
4. Bhatia R.; Garg S.; Attrid P.; Sol-Gel-Based Synthesis of Metal Oxide Nanoparticles for Air and Water Purification, *Smart Ceramics*., **2018**, *18*, 275-301 https://doi.org/10.1201/9781315163598-9
5. Patil S. S.; Patil S.; Patil D.K.; Kamble V. S.; Pawara J.M.; Synthesis, Spectral and Thermal Studies of Mixed Ligand Yt (III) Complexes and their Biological Investigation, *Indian Journal of Natural Sciences*., **2023**, *79*(14), 57847-57855 https://tnsroindia.org.in/JOURNAL/issue79/ISSUE%2079%20AUGUST%202023%20-%20FRONT%20PAGE%2001.pdf
6. Patil S. S.; Patil S.; Patil D.K.; Kamble V. S.; Pawara J.M.; *Synthesis of Metal Oxide Nanoparticles by Thermal Decomposition of a Ni(II) Complex and its Antimicrobial Activity, *Malaysian J. of Chemistry*., **2022**, *24*(3), 125-131 https://doi.org/10.55373/mjchem.v24i3.125
7. Pawara, J.; & Patil, S.; Synthesis Of Nio Nanoparticles By Thermal Decomposition At Low-Temperature Of New Aqua (2-Amino-6-Methyl Pyrimidine-4-ol And Isoleucine)Ni(Ii) Complex And Its Antimicrobial Study. *Journal of Advanced Scientific Research*., **2021**. *12*(03), 113-118. https://doi.org/10.55218/JASR.202112315
8. Larsen M. B.; Verdaguer M. P.; Schmidt B. F.; Bruchez, M. P.; Watkins S. C.; Alexander S.; Generation of endogenous pH-sensitive EGF receptor and its application in high-throughput screening for proteins involved in clathrin-mediated endocytosis *eLife*., **2019**, https://doi.org/10.7554/eLife.46135
9. James E Gomez, Benjamin B Kaufmann-Malaga, Carl N Wivagg, Peter B Kim, Melanie R Silvis, Nikolai Renedo, Thomas R Ioerger, Rushdy Ahmad, Jonathan Livny, Skye Fishbein, James C Sacchettini, Steven A Carr, Deborah T Hung (Ribosomal mutations promote the evolution of antibiotic resistance in a multidrug environment *eLife.,* **2019** https://doi.org/10.7554/eLife.20420
10. Jessica C.; Bo R. P.; Dai L.; Emrah θ Chaudhry W.; Minsu K.; Antibiotic-induced population fluctuations and stochastic clearance of bacteria *eLife*., **2018**, https://doi.org/10.7554/eLife.32976
11. Molly A Matty, Daphne R Knudsen, Eric M Walton, Rebecca W Beerman, Mark R Cronan, Charlie J Pyle, Rafael E Hernandez, David M Tobin Potentiation of P2RX7 as a host-directed strategy for control of mycobacterial infection. **2019** https://doi.org/10.7554/eLife.39123
12. Grinberg M.; Orevi, T.; Steinberg S.; Nadav K.; Bacterial survival in microscopic surface wetness *eLife* 8:e48508 **2019**, https://doi.org/10.7554/eLife.48508
13. Jennifer Hampton Hill, Eric A Franzosa, Curtis Huttenhower, Karen Guillemin A conserved bacterial protein induces pancreatic beta cell expansion during zebrafish development eLife 2016 5:e20145. https://doi.org/10.7554/eLife., 20145.
14. Molly A Matty, Daphne R Knudsen, Eric M Walton, Rebecca W Beerman, Mark R Cronan, Charlie J Pyle, Rafael E Hernandez, David M Tobin Potentiation of P2RX7 as a host-directed strategy for control of mycobacterial infection *eLife*., **2019,** *8*, e39123. https://doi.org/10.7554/eLife.39123
15. Brzyska, W.; & Ozga, W..; Thermal decomposition of yttrium and lanthanide complexes with mephenamic acid. *Thermochimica Acta*., **2020**, *195*, 149–155. https://doi.org/10.1016/0040-6031(92)80057-4

16. Brzyska, W..; & Oθga, W.; Preparation and properties of yttrium complexes with alkanodicarboxylic acids. J. of T. Analysis, 2018, 36(2), 441–453. https://doi.org/10.1007/bf01914498
17. Mishra, M. K.; Spectral Characrisation, Thermal Decomposition And Kinetic Study Of Chromium (Iii) Complexes With Salicylic Acid. *Rasayan J. of Chemistry*., **2018,** *11*(4), 1393–1398. https://doi.org/10.31788/rjc.2018.1143056
18. Mariane L. F.; Maryline B.; Enikθ M.; Olivier F.; David E.; Gyula T.; Carlos P.; Nicolas L.; Olivier Rousseaux, and *Raphaël Tripier Inorganic Chemistry*., **2018,** *57*(4), 2051-2063 DOI: 10.1021/acs.inorgchem.7b02953
19. Shijie D.; Paula L.; A switchable dimeric yttrium complex and its three catalytic states in ring opening polymerization, *Inorg. Chem. Front*., **2021**, *8*, 2088-2096 https://doi.org/10.1039/D0QI01479F
20. Chenyang L.; Yiyang Z.; Yttrium Oxide (Y_2O_3) Nanoparticle Crystallization in Gas-Phase Synthesis: A Molecular Dynamics Study. *Energy Fuels.,* **2021**, *35*(6), 5281–5290. https://doi.org/10.1021/acs.energyfuels.0c04090
21. Govindasamy R.; Govindarasu M.; Alharthi S.S.; Mani P.; Bernaurdshaw N.; Gomathi T.; Ansari M.A.; Alomary M.N.; Atwah B.; Malik M. S.; Rajeswari V.D.; Rekha K, Ahmed S. A.; Thiruvengadam M.; Sustainable Green Synthesis of Yttrium Oxide (Y_2O_3) Nanoparticles Using Lantana camara Leaf Extracts: Physicochemical Characterization, Photocatalytic Degradation, Antibacterial, and Anticancer Potency. *Nanomaterials (Basel)*., **2022,** *13*, 12(14):2393. doi: 10.3390/nano12142393.
22. Akhtar, Mohd & Ahamed, Maqusood & Alrokayan, Salman & Ramamoorthy, Muthumareeswaran & Alaizeri, Zabnallah. High Surface Reactivity and Biocompatibility of Y2O3 NPs in Human MCF-7 Epithelial and HT-1080 FibroBlast Cells. *Molecules*., **2020,** *25*. 1137. 10.3390/molecules25051137. https://www.ncbi.nlm.nih.gov/pmc/articles/PMC7179248/
23. Ahlam J. A.; Waleed M.; Al-Ogedy, Preparation and Characterization of Yttrium Oxide Nanoparticles at Different Calcination Temperatures from Yttrium Hydroxide Prepared by Hydrothermal and Hydrothermal microwave Methods, *Iraqi Journal of Science*., **2015**, *56*(2), 1572-1587. https://www.iasj.net/iasj/download/cdecd28eb119d010
24. Kwang-J.; Jeong and Dong-S.; B.; Synthesis and Characterization of Y2O3 Powders by a Modified Solvothermal Process, *Journal of Material Science.,* **2019**, *22*, 02,.http://dx.doi.org/10.3740/MRSK.2012.22.2.7
25. Govindasamy R.; Lebao M.; Ting B.; Wei W.; Shengfu W.; Thandapani G.; Nirmala G.; Maksim R.; Mohammad A. S.; Muthu T.; and Xiuhua Z.; Yttrium Oxide Nanoparticle Synthesis: *An Overview of Methods of Preparation and Biomedical Applications Appl. Sci*., **2021**, *11*, 2172. https://doi.org/10.3390/app 11052172
26. Mustafa A.; Mehdi G.; Ahmad N.; Golikand.; Taher Y.; Esmaeil Jangju1, yttrium Oxide Nanoparticles Prepared by Heat Treatment of Cathodically Grown Yttrium Hydroxide, International Scholarly Research Network ISRN Ceramics **2011**, Article ID 542104, 6 pages doi:10.5402/2011/542104